



HAL
open science

PolTimeSAR: Link between the measurement of a time series of N Jones vectors, and the measurement of a single Stokes vector integrating all these measurements. Application to (HH,HV) or (VH,VV) SAR time series

Elise Colin

► **To cite this version:**

Elise Colin. PolTimeSAR: Link between the measurement of a time series of N Jones vectors, and the measurement of a single Stokes vector integrating all these measurements. Application to (HH,HV) or (VH,VV) SAR time series. 2023. hal-04045501v1

HAL Id: hal-04045501

<https://hal.science/hal-04045501v1>

Preprint submitted on 24 Mar 2023 (v1), last revised 23 Aug 2024 (v2)

HAL is a multi-disciplinary open access archive for the deposit and dissemination of scientific research documents, whether they are published or not. The documents may come from teaching and research institutions in France or abroad, or from public or private research centers.

L'archive ouverte pluridisciplinaire **HAL**, est destinée au dépôt et à la diffusion de documents scientifiques de niveau recherche, publiés ou non, émanant des établissements d'enseignement et de recherche français ou étrangers, des laboratoires publics ou privés.

PolTimeSAR: Link between the measurement of a time series of N Jones vectors, and the measurement of a single Stokes vector integrating all these measurements. Application to (HH,HV) or (VH,VV) SAR time series

© Elise Colin

DTIS-Onera, Palaiseau, France, F-91123, Université de Paris Saclay, elise.colin@onera.fr

ABSTRACT

This paper addresses radar time series acquired with two polarization channels, one copolar and the other contrapolar. We show that the Eigenvalue decomposition of the coherence-covariance matrix of the complex Jones vectors contains the same information as the Stokes vector that would have been obtained by integrating all measurements into a single Stokes intensity measurement. We use two main parameters of this equivalent Stokes vector: its degree of polarization and its principal orientation. We then proposed two polarimetric decompositions: the "Equivalent-Stokes" representation, totally independent of the total intensity, and the "Polarimetric with main orientation" representation. We test these decompositions on the (HH,HV) Tandem-X, and (VV,VH) Sentinel-one time series of the same area.

Keywords time-series · change detection · permanent scatterer · coefficient of variation

With the advent of Copernicus Sentinel-1 images, radar time series are more and more frequently used for various functionalities, such as monitoring the dynamics of natural areas, detecting human activities or anomalies Colin Koeniguer and Nicolas [2020]. For all of these applications, polarimetry is information that can improve performance in the use of time-series Colin-Koeniguer et al. [2021], Koeniguer [2019], Ni et al. [2022], Denize et al. [2019], Antropov et al. [2017], Alonso González et al. [2020], Conradsen et al. [2016].

Polarimetry refers to the ability to transmit and receive signals in various polarizations. We can distinguish between the theoretical tools that describe the polarimetric state of a wave, both for the transmitted and the received wave, and the formalism that describes the polarimetric behavior of the object, i.e. its ability to transform a given polarization wave into a different one.

Most studies have focused on target analysis, which is possible with full polarimetry, i.e. with the acquisition of four polarimetric channels. They distinguish between the calculation of first order statistical parameters (such as Pauli parameters) and second order parameters, i.e. those requiring the calculation of a covariance matrix, involving second order moments, such as the well known polarimetric entropy parameter Cloude and Pottier [1997], and all physical decompositions such as Freeman-Durden Freeman and Durden [1993] or Yamaguchi decompositions Yamaguchi et al. [2011].

There are two main issues with the use of these theories:

- Fully polarimetric information is not often available, due to its technological cost. Thus, Sentinel-1 images are most often acquired in VV and VH polarization. Tandem-X images are most often acquired in dual polarimetric mode.
- The estimation of the second order parameters is mostly done by choosing samples in a spatial neighborhood of the considered pixel. This estimation is done at the expense of the resolution. Moreover, we have already seen that for some resolution ranges, this estimation method is not satisfactory, because the ergodicity hypothesis is not respected. Thus, for X-band data of metric type, it has already been seen that the calculation of the entropy in a spatial neighborhood leads to very bad results.

Here, we propose to study a formalism that allows to circumvent these two difficulties.

First, we restrict our study to the use of radar time series containing two polarimetric channels: a measurement in copolar polarizations, and a measurement in contrapolar polarizations. This includes Sentinel-1 images in (VH,VV) mode.

Next, we consider the time series as a statistical series containing N samples of the same measurement: this configuration is equivalent to considering a fixed emission polarization, and to observe N polarimetric states of the re-emitted wave.

The originality of the approach is threefold:

- We use the tools for analyzing the behavior of a wave, instead of considering the analysis of a target.
- The different statistical samples used in the study of this re-emitted polarimetric state are the different temporal samples. Thus, it is possible to distinguish random from deterministic behavior, without any spatial averaging.
- Considering the second order statistical parameters for these N measurements, we consider the formalism of the measurement of a single Stokes vector. This allows us to consider the modeling of the traditional optical measurement of a Stokes vector, as the integration of N deterministic Jones vectors.

In section 2, we explain the formalism of the covariance-coherence matrix of the re-emitted wave. We then propose to derive two main parameters: the randomness of the polarization designated by "polarization diversity" and the main orientation of the wave. We make these calculations explicit in a literal way, which allows a fast implementation from raw signals.

In a third section, we demonstrate the mathematical properties that allow us to link the measurement of a single Stokes vector, and that of a deterministic Jones vector computed as an eigenstate of the time series.

In section 4, we illustrate the previously introduced concepts, on Tandem-X and Sentinel-1 time series, by proposing two representations of the information in false colors. We conclude in section 5.

1 Polarimetric coherence-covariance matrix of the emitted wave

In this section, we consider the case of a time series for which we have two polarimetric channels, copolar and crosspolar. This is notably the case for the continental Sentinel-1 stripmap images (VV and VH), or for a time series of Tandem-X images in the (HH,HV) dual-polarimetric mode. In this case, the time series can be viewed as a succession of Jones vector of the scattered wave, for a wave emitted with a fixed polarization X. In each pixel, we consider observation vector of 2 rows and N columns that we call \mathbf{P} . Each column k of \mathbf{P} can be seen as the Jones vector acquired in response to an emitted wave, for a fixed polarization X, where E_x will be the component of the backscattered field parallel to X, and E_y will be the component of the backscattered field perpendicular to X:

$$\mathbf{P} = (\mathbf{p}^1, \dots, \mathbf{p}^k, \dots, \mathbf{p}^N) = \begin{pmatrix} E_x^1 & E_x^2 & \dots & E_x^k & \dots & E_x^N \\ E_y^1 & E_y^2 & \dots & E_y^k & \dots & E_y^N \end{pmatrix}, \quad (1)$$

In the case of Tandem-X data in HH and HV polarizations, we have $X=H$, and $E_x = S_{hh}, E_y = S_{hv}$. In the case of Sentinel-1 data, in VV and VH polarizations, we have $X=V$, and $E_x = S_{vv}, E_y = S_{vh}$.

Recall that each of the vectors (E_x, E_y) is a Jones vector, which describes a polarization ellipse of ellipticity ϵ and orientation ψ , by:

$$\tan(2\psi) = \frac{2|E_x||E_y|}{|E_x|^2 - |E_y|^2} \cos \delta, \quad \sin(2\epsilon) = \frac{2|E_x||E_y|}{|E_x|^2 + |E_y|^2} \sin \delta, \quad \delta = \arg(E_x E_y^*) \quad (2)$$

This polarization ellipse can be represented in a cartesian plane, it is a deterministic polarization. We can therefore, for a given pixel, consider the N polarization states received, as in the example given in 1:



Figure 1: Examples of 10 elliptic representations corresponding to N=10 (HH,HV) values in a given pixel.

The main idea is to consider our N acquisitions of these polarimetric states as a single but random polarization state, of which we will measure several properties.

For this, we will consider two different formalisms:

- the coherence-covariance matrix of the N Jones vectors
- the associated Stokes vector

1.1 The coherence-covariance matrix of the Jones vectors

In order to study the polarimetric properties of this wave, we can measure the coherence-covariance matrix of the wave, sometimes also called the polarization matrix in the Jones formalism Mandel and Wolf [1995]. This matrix is written:

$$\mathbf{C} = \frac{1}{N} \sum_{k=1}^N \mathbf{p}^k \mathbf{p}^{k\dagger} = \begin{pmatrix} \langle |E_x|^2 \rangle & \langle E_x E_y^* \rangle \\ \langle E_x^* E_y \rangle & \langle |E_y|^2 \rangle \end{pmatrix} = \begin{pmatrix} c_{11} & c_{12} \\ c_{21} & c_{22} \end{pmatrix} \quad (3)$$

where \dagger denotes the conjugate transpose, c_{11} and c_{22} are real numbers, and $c_{12} = c_{21}^*$.

By construction, this matrix \mathbf{C} is Hermitian. When the two receptions E_x and E_y are totally decorrelated, then the extra diagonal coefficients are zero. On the contrary, if they are very correlated, then the two extra diagonal coefficients are very high.

Expressed in the eigenvector basis, the matrix \mathbf{C} will have zero extradiagonal coefficients: the eigenvector basis is therefore the polarization basis where the signals are the most temporally decorrelated.

Because the matrix \mathbf{C} is a 2x2 hermitian matrix, it is possible to express literally the eigenvectors and the eigenvalues: if we let:

$$\delta = \sqrt{(c_{11} - c_{22})^2 + 4|c_{12}|^2}$$

Then the two eigenvalues are:

$$\lambda^- = (c_{11} + c_{22} - \delta)/2$$

$$\lambda^+ = (c_{11} + c_{22} + \delta)/2$$

with the corresponding relative unitary eigenvectors:

$$\mathbf{v}_- = v_{0-} \begin{pmatrix} \lambda^- - c_{22} \\ c_{12}^* \end{pmatrix}, \quad v_{0-} = \frac{1}{\sqrt{(\lambda^- - c_{22})^2 + |c_{12}|^2}}$$

$$\mathbf{v}_+ = v_{0+} \begin{pmatrix} \lambda^+ - c_{22} \\ c_{12}^* \end{pmatrix}, \quad v_{0+} = \frac{1}{\sqrt{(\lambda^+ - c_{22})^2 + |c_{12}|^2}}$$

such that:

$$\mathbf{C} = \lambda^- \cdot (\mathbf{v}_- \mathbf{v}_-^\dagger) + \lambda^+ \cdot (\mathbf{v}_+ \mathbf{v}_+^\dagger) \quad (4)$$

The two eigenstates describe the two depolarization axes that are most temporally decorrelated. \mathbf{v}_+ , associated with the largest eigenvalue, is the main state, the one that best describes the main polarization of the ensemble. They are represented for our starting example, on the figure 2.

1.2 Main eigenstate orientation

It is interesting to consider then the orientation of the maximum eigenstate, given by:

$$\tan(2\psi) = \frac{2|E_x||E_y|}{|E_x|^2 - |E_y|^2} \cos \delta \quad (5)$$

with:

$$|E_x| = \lambda_+ - c_{22}, \quad |E_y| = |c_{12}|, \quad \delta = \arg(c_{12}) \quad (6)$$

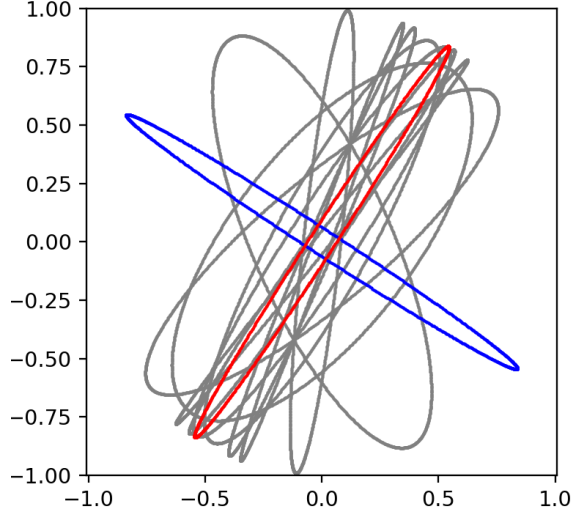


Figure 2: Superposition of the different eigenstates in gray, and representation of the two eigenstates: the most important in red, the second one in blue.

1.3 Scattering diversity of the covariance coherence matrix

We also propose to look at the distribution of the two eigenvalues, thanks to the coefficient Δ , calculated in the same way as the scattering diversity coefficient in Praks et al. [2009], either from the relative powers of the eigenvalues, or from the Froebenius norm of the coherence matrix:

$$\Delta = 2 - 2(p_1^2 + p_2^2) = 2 - 2\|\tilde{\mathbf{C}}\|_F^2 \quad (7)$$

where $p_i = \frac{\lambda_i}{\lambda_1 + \lambda_2}$, λ_1 and λ_2 are the two eigenvalues of \mathbf{C} , and $\|\cdot\|_F$ denotes the Froebenius norm, and $\tilde{\mathbf{C}} = \mathbf{C}/\text{trace}(\mathbf{C})$.

This polarimetric depolarization coefficient will have to be compared later with the notions of interferometric coherence, but note that no spatial averaging is required here, and that this parameter is independant from the total intensity.

2 The Stokes representation

The Stokes representation is particularly well suited to physical measurements, as it allows polarimetric states to be described directly from sums or differences of integrated intensities, easily measured in the optical domain Azzam et al. [1978]. Contrary to Jones vectors, Stokes vectors allow describing non-polarized or partially polarized states, in addition to fully polarized states.

And it is possible to express the Stokes vector as a function of the total intensity of the beam, its polarization rate, and parameters related to the shape of the polarization ellipse.

From the previous notations, it is written :

$$\mathbf{S} = \begin{pmatrix} \langle |E_x|^2 + |E_y|^2 \rangle \\ \langle |E_x|^2 - |E_y|^2 \rangle \\ \langle 2\Re(E_x E_y^*) \rangle \\ \langle 2\Im(E_x E_y^*) \rangle \end{pmatrix} = \begin{pmatrix} s_0 \\ s_1 \\ s_2 \\ s_3 \end{pmatrix} \quad (8)$$

where $\langle \cdot \rangle$ denotes the temporal average. We can see that these coefficients are directly related to the covariance-coherence matrix of the wave previously considered. Specifically, we have the following relationships:

$$\begin{cases} s_0 = c_{11} + c_{22} \\ s_1 = c_{11} - c_{22} \\ s_2 = c_{12} + c_{21} \\ s_3 = -j(c_{12} - c_{21}) \end{cases}, \begin{cases} 2c_{11} = s_0 + s_1 \\ 2c_{12} = s_2 + js_3 \\ 2c_{21} = s_2 - js_3 \\ 2c_{22} = s_0 - s_1 \end{cases} \quad (9)$$

A crucial parameter of the Stokes vector is the degree of polarization, which is defined as follows:

$$doP = \frac{\sqrt{s_1^2 + s_2^2 + s_3^2}}{s_0} \quad (10)$$

by writing:

$$(1 - \Delta) = 2\|\tilde{\mathbf{C}}\|_F^2 - 1 = 2\frac{c_{11}^2 + c_{22}^2 + |c_{12}|^2 + |c_{21}|^2}{c_{11}^2 + c_{22}^2} - 1 \quad (11)$$

which can be transformed, thanks to 9, into:

$$s_0^2(1 - \Delta) = s_1^2 + s_2^2 + s_3^2 \quad (12)$$

This leads to our first important result:

$$(1 - \Delta) = doP^2. \quad (13)$$

If we want to express the doP as a function of the initial data, this gives:

$$doP = \frac{2 \langle |E_x E_y^*| \rangle}{\sqrt{\langle |E_x|^2 \rangle^2 + \langle |E_y|^2 \rangle^2}} \quad (14)$$

The degree of polarization of the equivalent Stokes vector of our Jones vector time-series can be simply linked to the so-called scattering diversity defined from the coherence-covariance matrix of the Jones vectors.

We focus now on the ellipticity and orientation properties of this Stokes equivalent vector, to relate them to that of the principal eigenvector \mathbf{v}_+ .

If we reparameterize the unit eigenvector \mathbf{v}_+ using two complexes a and b , so that $\mathbf{v}_+ = (a, b)^t$, then the vector \mathbf{v}_- can be written $\mathbf{v}_- = (b^*, -a^*)^t$, and the matrix \mathbf{C} can be reparameterized thanks to the equation 4 by:

$$\mathbf{C} = \lambda^+ \begin{pmatrix} |a|^2 & ab^* \\ a^*b & |b|^2 \end{pmatrix} + \lambda^- \begin{pmatrix} |b|^2 & -ab^* \\ -a^*b & |a|^2 \end{pmatrix} \quad (15)$$

This means that the equivalent Stokes vector can be reparameterized thanks to Eq.9, by :

$$\mathbf{s} = \begin{pmatrix} \lambda^+ |a|^2 + \lambda^- |b|^2 \\ (\lambda^+ - \lambda^-)(|a|^2 - |b|^2) \\ (\lambda^+ - \lambda^-)2\Re(ab^*) \\ (\lambda^+ - \lambda^-)2\Im(ab^*) \end{pmatrix} \quad (16)$$

We recognize in the last three components, a part proportional to the last 3 components of the Stokes vector associated to the eigenvector \mathbf{v}_+ , with a proportionality factor $(\lambda^+ - \lambda^-)$ which is positive. This constitutes the proof of our second property:

The Stokes vector of the principal axis or eigenvector of the coherence-covariance matrix of the time series is collinear to the global Stokes vector. It therefore has the same orientation and ellipticity properties.

Fig. 3 represents different points on the Poincare sphere Deschamps and Mast [1973]: the different Jones vectors converted into measured Stokes vector appears in grey, as well as the Stokes vectors corresponding to both eigenvectors of the coherence-covariance matrix in blue and red. As the two eigenstates are orthogonal, we can see that the blue and

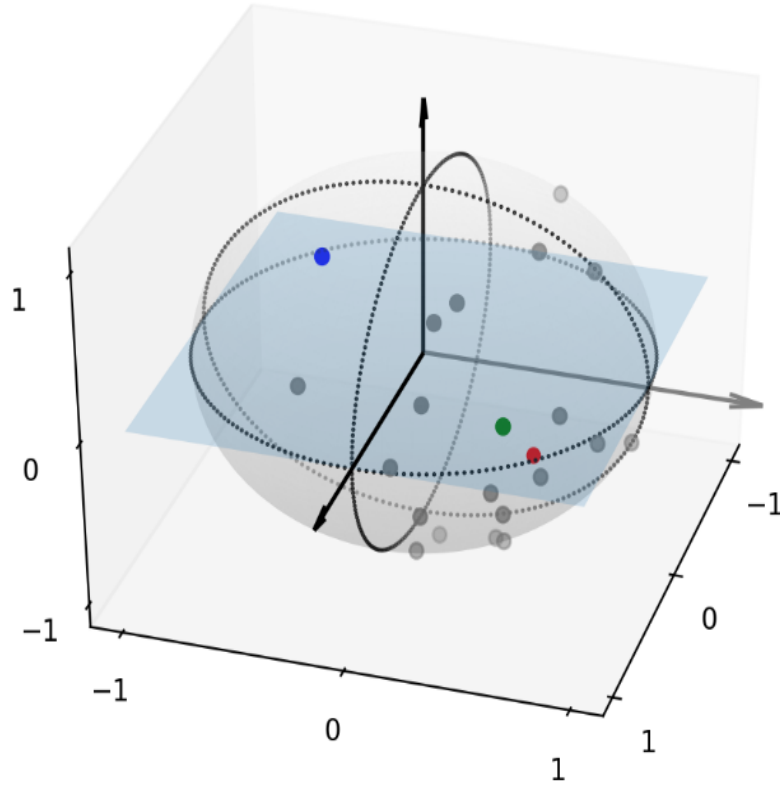


Figure 3: Example of representation on the Poincaré sphere: In gray, the N individual different Stokes vectors of the time-series; Red Point: Stokes vector of the main eigenvector, Blue Point: Stokes vector of the second eigenvector, Green point: Stokes vector for the whole time-series

red points are diametrically opposed on the Poincaré Sphere. The green point corresponds to the global Stokes vector, it is aligned with the blue and red points. Its norm is given by the degree of polarization.

To conclude this part, the eigenvector and eigenvalue decomposition of the coherence-covariance matrix of the time series contains the same information as the equivalent Stokes vector which would have consisted in integrating in time all the radar observations.

3 Proposition of two colored PolTimeSAR representations

In this section, we propose two colored representations exploiting the main features we found in the previous sections, namely the degree of polarization and the ellipse parameters of the main polarization.

3.1 A pure polarimetric representation: the "Equivalent-Stokes" time series representation

The first representation is a representation that exploits only the purely polarimetric information, making it independent of the total intensity notion.

For this one, we use the three parameters Δ , ϕ , and ϵ to make a false color representation of the stability of the temporal polarimetric information: we use the degree of polarization doP to code the brightness of the image (for a strongly temporally polarized pixel, the value will be high), we use the ellipticity to code the saturation (a saturated color corresponds to a linear polarization), and we use the orientation of the polarization to code the hue.

In figure 4, we show the result of this representation on Tandem-X images acquired in HH and HV polarizations for ten dates. These data have a resolution of 2 meters.

All the parameters of this representation are independent of the collected power, even though the deterministic targets appear with very low depolarizations, well contrasted with the natural areas. To better convince us, we show the channel corresponding to the polarization degree parameter at the top right of this figure.

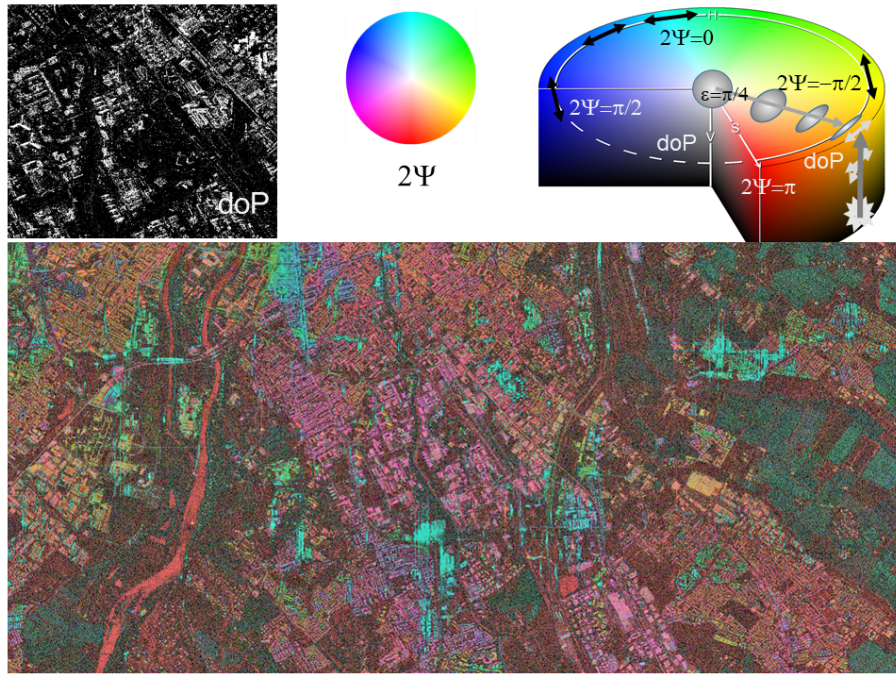


Figure 4: Pure polarimetric representation: the "Equivalent-Stokes" time series representation

3.2 The "Main-orientation polarimetric" representation

In the second representation, we use the average intensity to code the brightness. We use the degree of polarization to code color saturation. The hue always codes the same main orientation parameter.

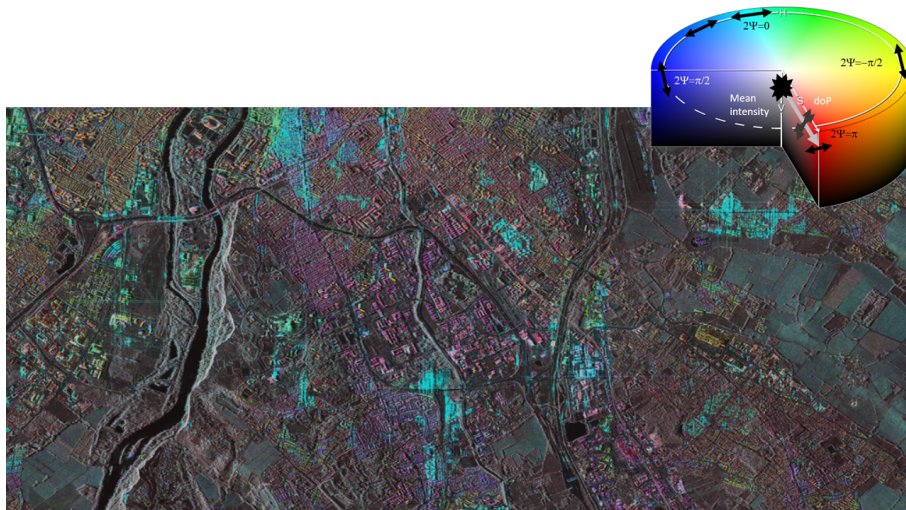


Figure 5: The "Main-orientation polarimetric" representation over Tandem-X data (Toulouse, France)

In figure 5 we show the result of this representation on previous Tandem-X data. We find the same trends as in figure 4, except for the areas of very low noise ratios where the polarimetric properties are almost no longer visible. A typical

example is the Canal du Midi, which has a high polarizing power aligned on the trajectory direction. In 5, we can no longer see this feature because the signal-to-noise ratio is too low.

We represent an extract of the global image footprint in figure 6. This one allows us to see the diversity of the orientations estimated on the deterministic targets.



Figure 6: The "Main-orientation polarimetric" representation: Extract on Tandem-X data (Toulouse, France)

We also applied our representation to a Sentinel-1 time series, for the same period and coverage, i.e. about 40 images in VV and VH polarizations. The result is shown in Figure 7. In the Sentinel-1 data, the contrast between deterministic and nondeterministic targets is less binary, much more nuanced, and the estimation of orientations appears narrower around the main acquisition orientations. This result suggests that, for this wavelength and resolution, the polarimetric behavior could be very different: several levels of depolarizations are involved, but there are fewer purely deterministic targets. We need to confirm this result with other data.

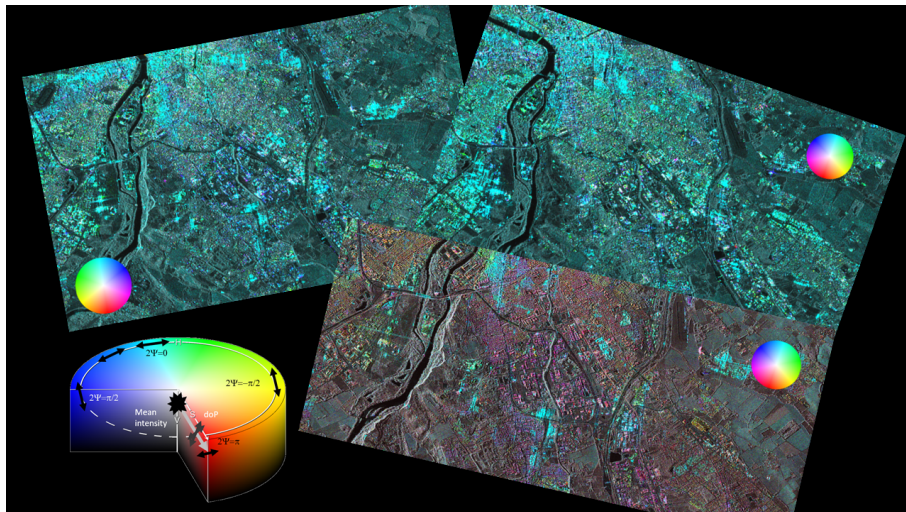


Figure 7: The "Main-orientation polarimetric" representation: comparison between Sentinel-1 ascending mode and Sentinel-1 descending, and Tandem-X data (Toulouse, France)

In figure 8, we zoomed in on an emblematic university building in Toulouse, called a tripod, because of the geometric distribution in three directions of the building. The image on the right is the optical view. In the colored composition,

we find the azimuthal orientations of these three buildings, with patterns on the roof that suggest that the backscatter has focused on some details with particular directions.

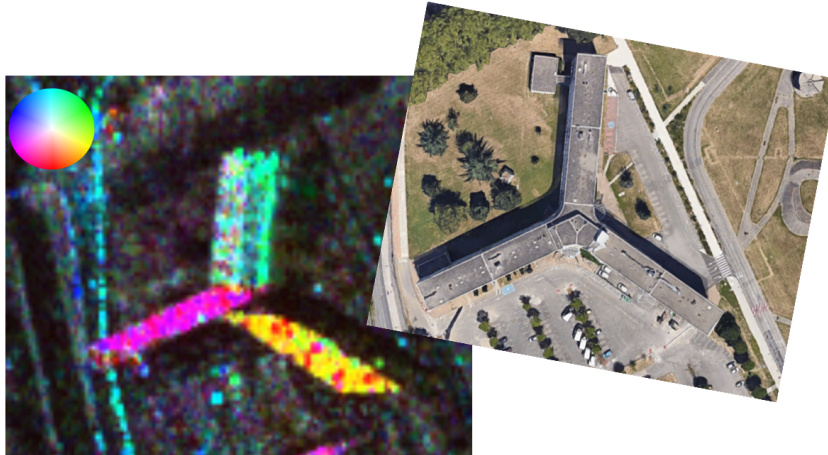


Figure 8: The "Main-orientation polarimetric" representation: Zoom on a particular building (Toulouse, France)

4 Conclusion

This paper concerns radar time series acquired with two polarization channels, one copolar and the other contrapolar. It proposes to consider these signals as a succession of Jones vector measurements to fully describe the polarization of the backscattered wave.

We show that the eigenvalue decomposition of the coherence-covariance matrix of these complex Jones vectors contains the same information as the Stokes vector that would have been obtained by integrating all measurements into a single Stokes intensity measurement. We use two main parameters of this equivalent Stokes vector: its degree of polarization, and its principal orientation.

We then proposed two polarimetric decompositions: the first relies only on purely polarimetric descriptors, made independent of the total intensity: ellipticity, orientation, and degree of polarization. We called this representation the "Equivalent-Stokes" time series representation.

A second color representation includes the degree of polarization, orientation, and total intensity. We called this decomposition the "Main-orientation polarimetric" representation.

Applied to the Sentinel-1 and Tandem-X time series over the same area, they show very different results for the two cases. The degree of polarization allows us to see strongly distinct behaviors on Tandem-X between deterministic and non-deterministic targets without using intensity information. The main orientations estimated seem to correspond to the azimuthal directions of the buildings or the deterministic targets.

Further investigations will be necessary to understand the role of wavelength and resolutions and the potential differences in behavior between (HH, HV) and (VV, VH) modes.

Acknowledgements

The TanDEM-X data were provided by DLR under the scientific proposal OTHER0103. This work would not have been possible without the collaboration of Paola Rizzoli and Jose Luis Bueso Bello in DLR, whom we thank very sincerely. This fruitful collaboration was initiated in the framework of the ONERA-DLR virtual research center for cooperation in "AI and applications in aerospace engineering."

On a personal note, I would like to thank Professor Eric Pottier for inviting me to address the polarization case of Sentinel-1 and for encouraging me to pursue the study of polarimetric time series under the acronym PolTimeSAR.

References

- Elise Colin Koeniguer and Jean-Marie Nicolas. Change detection based on the coefficient of variation in sar time-series of urban areas. *Remote Sensing*, 12(13):2089, 2020.
- Elise Colin-Koeniguer, Nicolas Trouve, Yoshio Yamaguchi, Yue Huang, Laurent Ferro-Famil, VD Navarro Sanchez, JM Lopez Sanchez, D Monells, R Iglesias, X Fabregas, et al. Urban applications. *Polarimetric Synthetic Aperture Radar: Principles and Application*, pages 215–254, 2021.
- Elise Colin Koeniguer. POL-timeSAR: Benefits of polarimetry on change detection in time-series. Communication presented during POLINSAR 2019 event: <https://polinsar2019.esa.int/files/presentation199.pdf>, January 2019.
- Jun Ni, Carlos López-Martínez, Zhongbo Hu, and Fan Zhang. Multitemporal sar and polarimetric sar optimization and classification: Reinterpreting temporal coherence. *IEEE Transactions on Geoscience and Remote Sensing*, 60:1–17, 2022.
- Julien Denize, Laurence Hubert-Moy, and Eric Pottier. Polarimetric sar time-series for identification of winter land use. *Sensors*, 19(24):5574, 2019.
- Oleg Antropov, Yrjö Rauste, Tuomas Häme, and Jaan Praks. Polarimetric alos palsar time series in mapping biomass of boreal forests. *Remote Sensing*, 9(10):999, 2017.
- Alberto Alonso González, Carlos López Martínez, Kostantinos Papathanassiou, and Irena Hajnsek. Polarimetric sar time series change analysis over agricultural areas. *IEEE transactions on geoscience and remote sensing*, 58(10):7317–7330, 2020.
- Knut Conradsen, Allan Aasbjerg Nielsen, and Henning Skriver. Determining the points of change in time series of polarimetric sar data. *IEEE Transactions on Geoscience and Remote Sensing*, 54(5):3007–3024, 2016.
- Shane R Cloude and Eric Pottier. An entropy based classification scheme for land applications of polarimetric sar. *IEEE transactions on geoscience and remote sensing*, 35(1):68–78, 1997.
- Anthony Freeman and Stephen L Durden. Three-component scattering model to describe polarimetric sar data. In *Radar Polarimetry*, volume 1748, pages 213–224. SPIE, 1993.
- Yoshio Yamaguchi, Akinobu Sato, Wolfgang-Martin Boerner, Ryoichi Sato, and Hiroyoshi Yamada. Four-component scattering power decomposition with rotation of coherency matrix. *IEEE Transactions on Geoscience and Remote Sensing*, 49(6):2251–2258, 2011.
- Leonard Mandel and Emil Wolf. *Optical coherence and quantum optics*. Cambridge university press, 1995.
- Jaan Praks, Elise Colin Koeniguer, and Martti T Hallikainen. Alternatives to target entropy and alpha angle in sar polarimetry. *IEEE Transactions on Geoscience and Remote Sensing*, 47(7):2262–2274, 2009.
- Rasheed MA Azzam, Nicholas Mitchell Bashara, and Stanley S Ballard. Ellipsometry and polarized light. *Physics Today*, 31(11):72, 1978.
- G Deschamps and P Mast. Poincaré sphere representation of partially polarized fields. *IEEE Transactions on Antennas and Propagation*, 21(4):474–478, 1973.